Rhythmic arm movements are less affected than discrete ones after a stroke

P. Leconte[1,5], J.J. Orban de Xivry[2,3,5,6], G. Stoquart[2,4,5], T. Lejeune[2,4,5], and R. Ronsse[1,2,5]

[1] *Université catholique de Louvain, Institute of Mechanics, Materials and Civil Engineering,* Place du Levant 2, 1348 Louvain-la-Neuve, Belgium *(patricia.leconte@uclouvain.be, renaud.ronsse@uclouvain.be)*

[2] *Université catholique de Louvain, Institute of Neuroscience,* Tour Pasteur - Avenue Mounier 53, 1200 Brussels, Belgium *(gaetan.stoquart@uclouvain.be, thierry.lejeune@uclouvain.be)*

[3] *Université catholique de Louvain, Institute of Information and Communication Technologies, Electronics and Applied Mathematics,* Avenue Georges Lemaître 4, 1348 Louvain-la-Neuve, Belgium *(*jean-jacques.orban@uclouvain.be*)*

[4] *Université catholique de Louvain, Cliniques universitaires Saint-Luc, Physical Medicine and Rehabilitation Department,* Brussels, Belgium

[5] *Université catholique de Louvain, Louvain Bionics, 1348* Louvain-la-Neuve, Belgium

[6] *KU Leuven, Department of Kinesiology, Movement Control and Neuroplasticity Research Group*, 3001 Heverlee, Belgium

---

Running head

Rhythmic vs. discrete movements after stroke

Address for correspondence

Patricia Leconte, *Université catholique de Louvain, Institute of Mechanics, Materials and Civil Engineering,* Place du Levant 2, 1348 Louvain-la-Neuve, Belgium *(patricia.leconte@uclouvain.be*)

Abstract

Recent reports indicate that rhythmic and discrete upper limb movements are two different motor primitives which recruit, at least partially, distinct neural circuitries. In particular, rhythmic movements recruit a smaller cortical network than discrete movements. The goal of this paper is to compare the levels of disability in performing rhythmic and discrete movements after a stroke. More precisely, we tested the hypothesis that rhythmic movements should be less affected than discrete ones, because they recruit neural circuitries that are less likely to be damaged by the stroke.

Eleven stroke patients and eleven age-matched control subjects performed discrete and rhythmic movements using an end-effector robot (REAplan). The rhythmic movement condition was performed with and without visual targets to further decrease cortical recruitment.

Movement kinematics was analyzed through specific metrics, capturing the degree of smoothness and harmonicity.

We reported three main observations: (i) the movement smoothness of the paretic arm was more severely degraded for discrete movements than rhythmic movements; (ii) most of the patients performed rhythmic movements with a lower harmonicity than controls; and (iii) visually guided rhythmic movements were more altered than non-visually guided rhythmic movements. These results suggest a hierarchy in the levels of impairment: discrete movements are more affected than rhythmic ones, which are more affected if they are visually guided.

These results are a new illustration that discrete and rhythmic movements are two fundamental primitives in upper-limb movements. Moreover, this hierarchy of impairment opens new post-stroke rehabilitation perspectives.

Keywords

Stroke, rhythmic movements, discrete movements, upper-limb, rehabilitation

Glossary

D-T: discrete task with small targets

FMA-UE : Fugl-Meyer assessment of the upper extremity

H : harmonicity index

ID : index of difficulty

PEAK: number of peaks in the velocity profile

LDJ : logarithmic dimensionless jerk

R-T : rhythmic task with large targets

R-NT: rhythmic task without targets

Introduction

Daily life motions of the upper limb are composed of complex combinations of rhythmic and discrete movements, e.g., wiping a table or playing the piano (Sternad and Dean 2003). Discrete movements are defined as movements between a succession of postures with zero velocity and acceleration, while rhythmic movements are periodic and display an acceleration peak at the zero-velocity movement reversal (Hogan and Sternad 2007; Goto et al. 2014). The literature reached a consensus stating that rhythmic and discrete movements form two different motor primitives (Guiard 1993; Schaal et al. 2000, 2004; Sternad et al. 2000; de Rugy and Sternad 2003; Spencer et al. 2003; van Mourik and Beek 2004; Buchanan et al. 2006; Smits-Engelsman et al. 2006; Hogan and Sternad 2007, 2012, 2013; Ikegami et al. 2010; Levy-Tzedek et al. 2010; Howard et al. 2011; Giszter 2015). In summary, discrete movements are not made of truncated rhythmic movements, and rhythmic movements do not consist of concatenated discrete movements.

Schaal et al. (2004) investigated the brain areas involved in producing simple discrete and rhythmic movements of the wrist via fMRI. They observed that discrete movements activated a variety of contralateral areas, such as BA7, BA40, BA44, BA47, PMdr, and RCZa, known to be involved in high-level computational processes, e.g., planning. Rhythmic movements, on the other hand, activated only a small number of unilateral sensorimotor areas (M1, S1, PMdc, SMA, pre-SMA, CCZ, RCZp, and cerebellum), most of which being also recruited in producing discrete movements.

After a stroke, both discrete and rhythmic movements are potentially affected (Gowland et al. 1992; Krebs et al. 1999; Rohrer et al. 2002; Dipietro et al. 2009; Hogan and Sternad 2009; Gilliaux et al. 2012, 2014a; Zehr et al. 2012; Simkins et al. 2013). However, to the best of our knowledge, no study has compared the levels of impairment between both movements in the same patients.

Consequently, in this paper, we tested the hypothesis that stroke would affect rhythmic task motor performance less than discrete task motor performance. Indeed, the stroke insult significantly impacts cortical areas, and the cortical network recruited in producing discrete movements is larger than for rhythmic movements. In addition, we tested the existence of a hierarchy in the levels of impairments after a stroke: patients with impaired rhythmic movements should have impaired discrete movements, but not vice versa. Indeed, if the cortical network activated in producing discrete movements is larger than the one for rhythmic movements (Schaal et al. 2004), some patients could be affected only in the production of discrete movements, if the circuitries governing rhythmic movements are left intact. The reverse picture is more unlikely, since impairment in producing rhythmic movements would reveal a disorder in the recruitment of unilateral sensorimotor areas being active during the production of both movement types. The main goal of the present paper is thus to *compare* the levels of impairment between discrete and rhythmic movements in the same post-stroke patients. To this end, stroke patients and healthy subjects were asked to perform simple back-and-forth movements with their upper limbs between two visual targets, once in a discrete way and once in a rhythmic way.

Finally, a third movement type was added, i.e., a non-visually guided rhythmic task where participants were asked to make rhythmic movements without receiving visual targets. Our objective was to test whether this task would be differently affected than the one with visual targets. Indeed, the presence of visual targets requires more planning and leads to possible movement corrections by the visuomotor pathways (Desmurget et al. 1999, 2001; Hanakawa et al. 2008; Andersen and Cui 2009; Glover et al. 2012), hence reinforcing the dependence on cortical networks. Therefore, removing the visual targets should facilitate the task and further isolate possible subcortical and/or spinal contributions.

In sum, the present paper aims to establish whether there exists a hierarchy of impairment in different motor tasks after a stroke by comparing the levels of impairment of (1) non-visually guided rhythmic movements, (2) visually guided rhythmic movements, and (3) visually guided discrete movements between stroke patients and healthy controls.

Materials and Methods

Participants

Eleven stroke patients and eleven age-matched control subjects were included in this study. Stroke patients were ineligible for this study if they suffered from: (i) any other disorder affecting the upper limb; (ii) severe visual impairments or severe neuropsychological impairments like aphasia, attention deficit disorder, or neglect; (iii) a cerebellar stroke; or (iv) an active elbow range of motion smaller than 20°. To assess the sensorimotor function of the upper limb, stroke patients were evaluated with the Fugl-Meyer Assessment of the upper extremity (FMA-UE) (Fugl-Meyer et al. 1974); this scale quantifies the level of impairment, with an index ranging from 0 to 66 points. The FMA-UE score and other relevant characteristics of the patients and control participants are presented in Table 1.

Before beginning the experiment, all participants gave their written informed consent to participate to the study, which was approved by the scientific and ethical committees of the Université catholique de Louvain.

Measurement device

The experiments were performed by using the REAplan, an upper-limb end-effector research prototype robot developed within our university. The REAplan was initially designed to quantify the upper limb impairments of disabled patients (Gilliaux et al. 2012, 2014a) and to provide robot-assisted therapies to the same populations (Gilliaux et al. 2014b).

The robot is composed of (i) a height-adjustable, horizontal table, (ii) a handle equipped with force sensors that are held by the participant, (iii) two motors actuating the handle along the orthogonal directions in the horizontal plane, (iv) a flat screen and loudspeakers in front of the participant, which can provide visual feedback of the position of the handle and any other visual or auditory information, and (v) an interface for the therapist. Most of these components can be seen in Fig. 1(top).
During the tasks, data were recorded at 125Hz for off-line analyses.

Experimental procedure

Participants were seated on a chair or their own wheelchair in front of the device. The height of the REAplan was adjusted such that the elbow formed a right angle and the arm was in a neutral position along the trunk when the participant held the handle in its initial position. Seven patients were strapped to the handle when performing the task with their paretic arm because their hand was too weak to hold it. For seven patients, their trunks were strapped to the chair because they made compensatory movements during the training phase.

All participants performed three tasks with each of their arms. All tasks consisted of performing back-and-forth movements restricted to a straight trajectory in the forward-backward direction of motion (sagittal plane). Lateral movements were thus prohibited by implementing stiff virtual walls with the device, while the direction of motion was controlled under a "free-mode" (or transparent) admittance controller.

Each task consisted of the achievement of three trials of fifteen back-and-forth movements at self-selected speed, i.e., forty-five back-and-forth movements per task per arm. Two patients out of eleven (patients 2 and 10) were too weak to fulfill three trials with their paretic arm and thus only performed two trials. Participants received visual feedback that mapped the position of the handle on the screen during all tasks.

The first two tasks consisted of making back-and-forth movements between two green rectangular targets (Fig. 1, a and b), with the instruction to make the movement reversal (i.e., to reach zero velocity) inside the target. Once the handle reached the target, it turned red and a beep was delivered; this gave visual and auditory feedback for reversing the movement direction.

The only differences between the first two tasks were the width and distance between the targets, determined according to the so-called "index of difficulty" (ID) (Guiard 1993; Buchanan et al. 2006), based on Fitts' law (Fitts 1954):

$$ID = \log_2 \frac{2A}{W},$$

where A denotes the movement amplitude and W is the target's width (Fig.1a). This index thus captures that it is more difficult to make longer movements and aim at smaller targets. Researchers (Guiard 1993; Buchanan et al. 2006) showed that healthy participants perform kinematically discrete movements with zero acceleration at the movement reversal when the ID is large. When the ID is smaller, the same authors further showed that healthy participants perform kinematically rhythmic movements, with maximal acceleration (in absolute value) at the movement reversal.

In the present study, the movement amplitude A was set to 12.5 cm and the target width W was set to 0.7 cm for the first task (ID = 5.16; pilot tests showed this ID was large enough to induce discrete movements with the present task). For the second task, A was set to 10.5 cm and W was set to 3.5 cm (ID = 2.58). The position cursor, provided as visual feedback, had a diameter of 0.5 cm. All patients had active ranges of motion larger than these amplitudes.

During the third task, no rectangular target was visible on the screen, and the participants were instructed to make movements of similar amplitudes as during the other tasks. They were instructed to imagine that they were sawing wood to induce kinematically rhythmic movements; no auditory feedback was delivered during this last task. The three tasks were thus "discrete with targets" (D-T), "rhythmic with targets" (R-T), and "rhythmic with no target" (R-NT); see Fig. 1.

Before starting each block of trials, participants were trained for each task for approximately one minute, until obtaining consistent movements. The first six subjects and patients performed the tasks in the following order: R-T, R-NT, and D-T, first with their right or healthy arm and then with their left or paretic arm. The remaining five subjects and patients performed the tasks in the reverse order: D-T, R-NT, and R-T, with their left or paretic arm first.

Data processing and kinematic indices

The raw position trajectories of the handle were filtered using a forward and backward second-order Butterworth filter with a cut-off frequency of 6 Hz. Thereafter, the velocity, acceleration, and jerk (third derivative) of the handle were obtained by successive numerical differentiation of the position profile.

All trials were then cut into individual movements between the locations of the zero velocity points at the movement reversal. Each movement thus corresponded to an individual discrete movement or to a half-cycle of a rhythmic movement.

General performances of the tasks, i.e., mean velocity (v_{mean}), movement amplitude (A), and precision at the movement reversals, were computed. The precision at the movement reversal was computed as 1 standard deviation of the distribution of the absolute error between the handle position at movement reversal and the location of the target center. This metric thus captures the distribution of reversal points around their average and was computed only for the D-T and R-T conditions, where visual targets were displayed.

Next, dwell time in individual movements was computed to assess the kinematic difference between discrete and rhythmic movements. Dwell time was introduced in the literature as a specific landmark of discrete movements (Buchanan et al. 2006; Hogan and Sternad 2007; Sternad et al. 2013); it corresponds to the duration around movement reversal between the first time the velocity gets below 5% of the velocity peak of the preceding movement and the first time it gets above 5% of the velocity peak of the following movement (Fig. 2). Note that, with this definition, an ideal sinusoidal movement displays a dwell time of about 3.2% of the cycle duration.

Finally, the following movement kinematic indices were computed for each individual movement to assess their harmonic nature and smoothness.

1. Harmonicity index H (Guiard 1993; Buchanan et al. 2006): This metric captures the movement nature, i.e., whether it is a rhythmic movement (maximal acceleration at the movement reversal) or a discrete movement (zero acceleration at the movement reversal). It is computed by selecting a time window around the movement reversal, i.e., the second half of the preceding movement (before movement reversal) and the first half of the following movement (after movement reversal). In this time window, the acceleration is extracted and multiplied by the sign of its mean value to force the mean to be positive. Therefore, the maximum acceleration a_{max} (Fig. 2) is also positive. If a single peak occurs in this acceleration profile, *H* is set to 1. If several acceleration peaks occur, *H* is set to

$$H = \max\left(\frac{a_{min}}{a_{max}}, 0\right),$$

where a_{min} is the smallest acceleration value in the window between the first and the last acceleration peak (Fig. 2). If a_{min} is negative, then *H* is equal to 0. Since an ideal rhythmic movement is sinusoidal, its acceleration peak occurs at the movement reversal and *H* is thus equal to 1. An ideal discrete movement has a minimum jerk profile and thus acceleration is equal to zero at movement reversal; the corresponding *H* is equal to 0. Any post-stroke effect affecting the smoothness of discrete movements will thus be hardly visible with this index, which saturates to 0 for both smooth and non-smooth discrete movements. Consequently, the *H* index is reported for all tasks, but the statistical analysis mainly focuses on both rhythmic ones.

2. PEAK: this smoothness metric gives the number of peaks in the movement velocity profile. It was already used by several authors to analyze discrete movements after a stroke (Cirstea and Levin 2000; Kamper et al. 2002; Rohrer et al. 2002).

This metric is valuable because it is not sensitive to the movement type; indeed, the number of velocity peaks of both rhythmic and discrete movements is ideally equal to 1 for healthy subjects, disregarding corrective sub-movements which may happen close to movement reversal (Fig. 2). Consequently, this metric was independently computed in the zone of movement reversal and in the central phase of the movement. This measure provides an understanding of whether the differences observed between the different movement types and populations (patients vs. control) were due to changes in the final corrective sub-movements or in the central transport phase of the movement. These two zones were separated based on movement amplitude rather than on movement timing: the initial 25% and final 25% of the total movement amplitude were considered as the regions of movement reversal. Therefore, the central phase was taken as the centered 50% of the total movement amplitude (see Fig. 3 for examples of typical trials).

<ins>*3. Logarithmic dimensionless jerk (LDJ):*</ins> This jerk-based smoothness metric was validated for discrete movements performed by healthy and stroke patients (Balasubramanian et al. 2012). The main feature of this particular jerk-based smoothness metric is that it is not sensitive to the movement amplitude and duration and does not have a ceiling effect, like the dimensionless jerk (Hogan and Sternad 2009):

$$LDJ = \log\left(\frac{D^3}{v_{mean}^2} \int |j(t)|^2 dt\right),$$

with *D* being the movement duration and *j(t)* the movement jerk (Fig. 2). The smoother the movement is, the lower the *LDJ* value.

This metric is, nevertheless, sensitive to the movement type. An ideal rhythmic movement corresponds to a portion of the sinus (Hogan and Sternad 2007), so that the corresponding *LDJ* should be equal to 4.1. An ideal minimum-jerk discrete movement should have a bell-shaped velocity profile (Hogan and Sternad 2007) with a *LDJ* equal to 6.

We explored normalizing the LDJ metric according to these expected values (4.1 or 6) to make the metric insensitive to the movement type. We decided to not do this because we observed that this reduces the information that can be retrieved from the LDJ metric. Indeed, reporting a LDJ metric between 4.1 and 6 in a rhythmic task can capture (i) a movement performed with a non-ideal smoothness (i.e., a rhythmic movement with more than one velocity peak) or (ii) a smooth movement performed with a lower harmonicity, i.e., more like a healthy discrete movement. Therefore, the three metrics provide complementary information and must be analyzed in parallel. In particular, the PEAK metric will increase in the case of non-ideal smoothness of movement (particularly during the central movement phase), but not in movements with lower harmonicity.

Importantly, note that both of the smoothness indices we selected (PEAK and LDJ) were developed to measure smoothness without being sensitive to movement speed or amplitude.

All the above computations were performed using Matlab 7.10.0 R2010a (The MathWorks Inc, Natick, MA).

Data Analysis and Statistics

For all trials, the first five movements were excluded from analysis to avoid transient phenomena. In addition, this further excluded the first rhythmic cycles, which might be governed by the discrete primitive (van Mourik and Beek 2004; Howard et al. 2011).

Statistics were performed with JMP 10.0.0 software (SAS Institute Inc.).

We first analyzed the learning effect between the three trials for both groups and the lateralization effect between the dominant and non-dominant arms of the control group. Therefore, a mixed model that included the factors "group (patient and control)", "arm (dominant/non-paretic and non-dominant/paretic)", "task (D-T, R-T and R-NT)" ,"trial" , the two-factors interactions and the "participant number" as random effect to take into account the repeated structure of the dataset, was analyzed. The equation of this model is provided as supplementary material. It contained 11 variables: the 4 factors, the corresponding 6 two-factors interactions, and the bias. This model was solved using a "Restricted Maximum Likelihood" method to estimate the variance parameters. No learning effect was observed, either in the control or in the patient group, in the sense that no significant effect was found with the factor "trial" or its interactions in all metrics (all p-values > 0.05). Similarly, no laterality effect was found in the control group, i.e., the interaction "arm – group" was significant in all metrics and the post-hoc Tukey HSD tests did not show a significant difference between the dominant and non-dominant arms in the control group (all p-values > 0.05).

Consequently, for the subsequent analyses, the data were simplified by pooling the three trials together, and the dominant and non-dominant arms together in the control group. Therefore, for each task, a single mean value was kept for every metric for the paretic and non-paretic arms in the patient group and only one value per metric and per task in the control group.

We did not perform a 3 (arm) x 3 (task) analyses on this dataset, as it would have mixed intra- and inter-subject data in the "arm" factor (including the paretic and non-paretic arms of the stroke group, and a single arm from the control group). Therefore, three independent mixed models were performed on the simplified dataset for all the above-mentioned metrics over (i) the paretic side vs. control data, (ii) the non-paretic side vs. control data, and (iii) the paretic side vs. non-paretic side. Each model contained the following effects: the task (D-T, R-T, R-NT), the arm (two among paretic, non-paretic, and control), their interaction, and the participant number that was used as a random effect. Note that the degrees of freedom were different in models (i) and (ii) vs. model (iii) since the later was an intra-subject analysis while the formers were inter-subject analyses. The models were solved using a "Restricted Maximum Likelihood" method to estimate the variance parameters. Post-hoc Tukey HSD test was used to compare the modalities of significant factors.

In order to account for the potential increase in type I error due to the multiplicity of tests, the significance level was adjusted with a Bonferroni correction to p=0.017 (Dagnelie 2013).

Classification of the smoothness impairment of patients

To further classify the patients, the movement smoothness performed by the paretic arm of each patient was compared to the healthy control group. The PEAK and LDJ metrics were selected for this analysis. For both metrics, a patient was considered affected for a particular task if the corresponding metric value was above the mean value of the control group plus *x* standard deviation(s) of the control group value for the same metric. To test sensitivity effects with respect to the threshold being used, *x* was varied from 0.5 to 2. As such, patients could be classified into several groups according to two different metrics, i.e., patients affected in the R-T task, patients affected in the R-NT task, and patients affected in the D-T task. This analysis was performed first in the PEAK metric computed over the total movement duration, and then in the same metric restricted to the central movement phase. This permitted us to exclude possible sub-movements in the target reaching phase and focus on possible impairments restricted to the central transportation phase, which should be similar across movement types.

Results

1. Typical traces and general performances

Figure 3 shows typical traces of a healthy subject on the left and a stroke patient on the right for a rhythmic task (R-T, upper row) and for a discrete task (D-T, lower row). The healthy control subject (left column of Fig. 3) displayed the expected acceleration peak at the movement reversal of rhythmic movements and zero acceleration at the movement reversal during the discrete task. Both the rhythmic and discrete movements of the stroke patient were affected (right column of Fig. 3). However, observing the velocity profiles reveals a fundamental difference in the way the hemiparesis affected rhythmic and discrete movements: while this patient displayed more than one velocity peak per discrete movement, he managed to keep a single peak for the rhythmic movements.

Figure 4 (four upper panels) shows the general performances during the three tasks at the population level. In both healthy subjects and patients, discrete movements were performed with a lower velocity than rhythmic movements (task effect paretic vs. control: $F_{(2,40)}$=65.5; paretic vs non-paretic: $F_{(2,50)}$ =66.7; and control vs non-paretic: $F_{(2,40)}$=120.5 where all p's < 0.0001, and Tukey HSD, R-NT > R-T > D-T with all p's < 0.0001); this is consistent with Fitt's law (Guiard 1993; Buchanan et al. 2006; Sternad et al. 2013).

The mean amplitudes were 12.7 (SD 0.6) cm in the D-T task, 10.4 cm (SD 1.1) in the R-T task, and 13.4 cm (SD 2.9) during the R-NT task, with no significant differences between the groups (paretic vs non-paretic: $F_{(1,50)}$=0.85, p= 0.35 ; paretic vs control: $F_{(1,20)}$ = 0.49, p = 0.49; and control vs non-paretic: $F_{(1,20)}$= 2.9, p = 0.1).

As expected, dwell times were significantly higher during the discrete task than during both rhythmic tasks (exercise effect in control vs. non-paretic arms ($F_{(2,40)}$=58.1, in paretic vs. control $F_{(2,40)}$=13.8, and paretic vs. non-paretic $F_{(2,50)}$=6 with all p's < 0.0001 and Tukey HSD R-T vs D-T: p < 0.0001 and Tukey HSD R-NT vs D-T: p < 0.0001), which confirms that the tasks were executed as expected, i.e., with longer dwell times during the discrete task. Moreover, the reported dwell time in both rhythmic tasks was around 40ms, i.e. about 3% of the total movement duration, corresponding thus to an ideal sinusoidal movement (see methods).

The D-T task was performed with significantly longer dwell times by the patients with their paretic arm, as compared to their non-paretic arm or to the healthy group (all p's < 0.0001). This was not observed in the R-T and R-NT tasks.

Furthermore, the D-T task was performed with lower precision by the patients with their paretic arm, as compared to their non-paretic arm or to the healthy group (all p's < 0.0001). This was again not observed in the R-T task, while this metric was not computed for the R-NT task due to the absence of visual targets (see methods). Note finally that the level of precision was better for the discrete than the rhythmic task in both the control group and the non-paretic arm of patients. The decrease of precision in the D-T task reported for the patients' paretic arm brought it to the level of performance of the control group in the R-T task, i.e. about 0.7cm.

2. Stroke spares the smoothness of rhythmic movements

The observation reported above for a single patient – that rhythmic and discrete movements are differentially affected – is confirmed at the population level for both smoothness metrics (Fig. 4, bottom). First of all, for both measures of smoothness (LDJ and PEAK), movement smoothness was lower for the paretic arm of patients compared to their non-paretic arm and to the arms of age-matched healthy controls. This difference was stronger for discrete movements than for rhythmic movements (interaction between group and tasks, see Table 2). In all cases, this interaction indicated that the effect of group was higher in the discrete task than in any of the two rhythmic tasks (Table 2). In contrast, movement smoothness of the non-paretic arm appeared to be preserved in stroke patients in all tasks (interaction between group and tasks: PEAK: $F_{(2,40)} = 0.28$, $p = 0.76$; and LDJ: $F_{(2,40)} = 0.69$, $p = 0.51$).

We further investigated whether the above-mentioned effects were due to movement changes during the central part of the movement – which is supposed to be very similar across conditions – or during the reversal phase, i.e., where rhythmic and discrete movements are intrinsically different due to the need for stopping in discrete movements. Consequently, the velocity peak metric was independently computed during the central and reversal phases of the movement (Fig. 4). As expected, results show that, for the control group, the central phase of the movements was characterized by a single velocity peak. In contrast, the smoothness of the movements during the reversal phase differed as a function of the movement type: virtually no corrective sub-movement was performed during the rhythmic conditions, while about one corrective sub-movement was performed for every three discrete movements. Results further show that the movement smoothness of the patients' paretic arm was altered in both phases of the movement: more than one velocity peak was often observed during the central movement phase, while some extra velocity peaks were often observed during the reversal phase. Again, the difference in movement smoothness, compared to the healthy and non-paretic arm groups, was larger in the discrete task (statistics are given in Table 2). Finally, no difference was found between the non-paretic arm group and the control group, either in the central phase of the movement (factor arm non-paretic vs. control group: PEAK: $F_{(1,20)} = 2.7$, $p = 0.12$) or in the movement reversal phase (factor arm non-paretic vs. control group: PEAK: $F_{(1,20)} = 0.03$, $p = 0.87$). In sum, during discrete movements, the smoothness during both the central and reversal phases of the movements was affected by stroke.

3. Stroke affects the harmonicity of rhythmic movements

The harmonicity metric measures the movement continuity at movement reversal. If the subject stops, this index is equal to zero while perfect (sinusoidal) reversal would be associated with an index of 1. In agreement with the existing literature (Guiard 1993; Marder and Bucher 2001), our healthy control group showed an harmonicity index close to 1 in both rhythmic tasks and a harmonicity index close to zero in the discrete task (Fig. 5).

The trace of patient 7 in Fig. 3 shows that the rhythmic movements were not continuous (i.e. the harmonicity index during the rhythmic task was reduced); this observation can also be extended to the population level. In both rhythmic tasks, the paretic arm of the patients had a lower harmonicity index than in the control and non-paretic arm groups, although harmonicity index was higher in the R-NT task than in the R-T task. Both factors, task and group, had a significant effect (control vs. paretic: factor "task": $F_{(2,40)}$=100.1, p<0.0001, factor "group": $F_{(1,20)}$=9.6, p=0.0057 and no interaction: $F_{(2,40)}$=3.7, p=0.034; paretic vs. non-paretic: factor "task" : $F_{(2,50)}$=72, p<0.0001 with R-NT > R-T, p=0.02, R-T>D-T, p<0.0001; factor "group": $F_{(1,50)}$=14.4, p=0.0004 and no interaction: $F_{(2,50)}$=1, p=0.37). Again, the non-paretic and healthy arms exhibited similar harmonicity index in both rhythmic tasks (factor "task": $F_{(2,40)}$ = 142.3, p<0.0001; factor "group": $F_{(1,20)}$ = 1.80, p=0.19, interaction: $F_{(2,40)}$ = 0.8, p=0.44).

4. Absence of visual cueing induces better performances in rhythmic movements

We already illustrated that a lack of visual targets led to a less-degraded harmonicity index (Fig. 5). Namely, the harmonicity index of the paretic arm was lower than the non-paretic and healthy arms in both rhythmic tasks, but the harmonicity index was higher in the R-NT task than in the R-T task. Moreover, the LDJ metric revealed that the smoothness was not different between the paretic and non-paretic arm in the R-NT task (see LDJ row of Table 2), but well in the R-T task.

This confirms that rhythmic movements of the paretic arm were less affected when no visual guidance was given to the patient. A similar observation can be reported when comparing the paretic vs. control group, although in this case the significance threshold was not reached in any of the rhythmic tasks.

5. Hierarchy in the motor impairments

Our data suggest that a discrete task was more affected than a rhythmic task after stroke and also that a visually guided rhythmic movement was more impaired than a non-visually guided rhythmic one. In this section, we report a final analysis on the PEAK and LDJ metrics, which was conducted to classify the patients into groups in order to identify a possible hierarchy in the impairments. To establish this classification, a patient was considered "impaired" in a specific task and according to a given metric if it was larger than '*x*' standard deviation(s) above the mean value from the control group (Fig. 6). The classification displayed in Figure 6 (a, c, and e) was built with x=1.

This analysis highlights the existence of a hierarchy: a patient who was impaired in the R-NT task was also impaired in the R-T and D-T tasks, and a patient who was impaired in an R-T task was also impaired in the D-T task. No patient was only affected in a rhythmic exercise and nobody was only affected in the R-T or R-NT tasks. Finally, some patients were affected in none of the tasks, according to our metrics. These are the patients being displayed out of the Venn diagram (two in Fig. 6a and c, and three in Fig. 6e).

To analyze the sensitivity of this hierarchy to the SD threshold (parameter x), this threshold was varied from 0.5 to 2 times the standard deviation (SD) of the control group (Fig. 6b, d, and f). This analysis revealed that the identification of the hierarchy was insensitive to the threshold being used. Finally, this analysis was refined by keeping only the number of peaks in the central phase of the movement (Fig. 6, e and f), which is ideally made of a single velocity peak and disregards all corrective sub-movements close to the reversal zones; similar results were obtained. In this case, eight patients were identified as affected in the D-T task, among which only one was affected in the R-NT task.

Discussion

The objective of the present study was to quantify the level of impairment in producing visually guided discrete, visually guided rhythmic, and non-visually guided rhythmic movements with the upper limbs after a stroke. We found that: (i) stroke preferentially affects the smoothness of discrete movements, not rhythmic movements; (ii) stroke affects the harmonicity of rhythmic movements; and (iii) patients who were affected in producing rhythmic movements were all affected in producing discrete movements, but not the other way around, i.e., there was a hierarchy of impairment: a patient affected in a rhythmic task was always affected in the discrete task, and a patient affected in a non-visually guided rhythmic movement was always affected in the visually guided rhythmic movement.

Both rhythmic and discrete movements are affected by stroke, but not to the same extent

Results showed that the movement smoothness of the patients' paretic arm was altered for both rhythmic and discrete movement production. However, the difference in movement smoothness compared to the healthy and non-paretic arm was larger in the discrete task than in the rhythmic one. This was, for instance, quantified with the LDJ metric. This metric was reported to be insensitive to the movement amplitude or timing, but sensitive to the movement type: a perfect rhythmic movement should have a sinusoidal profile with a LDJ of 4.1, and a perfect discrete movement should display a bell-shaped velocity profile with a LDJ of 6. This is critical for the performance analysis during the rhythmic task. Indeed, as explained in the methods, a LDJ metric between 4.1 and 6 during the production of rhythmic movements can be due either to a decreased smoothness or to a lower harmonicity (i.e., a movement with longer dwell-time, like a discrete one). This last case was observed for the paretic arm in both rhythmic conditions, where the amount of velocity peaks was not different across the groups in both the central and reversal portions of movements. Therefore, the reported increased LDJ value in the paretic arms during both rhythmic tasks (reaching significance only for the R-T task) can only be due to a lower harmonicity and not to a decreased smoothness. This result was confirmed by the analysis of the harmonicity index: rhythmic movements with the paretic arm were produced with a decreased harmonicity with respect to the control group. In sum, discrete movements were affected in the sense that the patients performed them in a less smooth way, i.e. with more velocity peaks, while rhythmic movements were affected in the sense that the patients performed them in a less harmonic way, i.e., resembling the discrete movements of the control group.

Post-stroke behavior suggests that discrete and rhythmic movements form two different primitives

We reported an impairment hierarchy, namely that the rhythmic task was not affected for some patients being affected in the discrete task, and that this impairment was visible in both the central transportation and reversal phases of the movement. This is in line with the theory postulating that rhythmic and discrete movements are, at least partially, controlled by distinct neural circuitries (Guiard 1993; Schaal et al. 2000, 2004; Sternad et al. 2000; de Rugy and Sternad 2003; Spencer et al. 2003; van Mourik and Beek 2004; Haiss and Schwarz 2005; Buchanan et al. 2006; Smits-Engelsman et al. 2006; Hogan and Sternad 2007, 2012, 2013; Ikegami et al. 2010; Levy-Tzedek et al. 2010; Howard et al. 2011; Giszter 2015). A discrete movement is not a truncated rhythmic movement, i.e., discrete movements are not based on the use of the rhythmic movement primitive. Moreover, if rhythmic movements were based on a concatenation of discrete movements, rhythmic movements should be affected in the central phase of the movement, similar to the discrete task. Indeed, if both movements shared the same neural representation, both movements should be equally affected (Nozaki et al. 2006). This suggests that discrete and rhythmic movements form two different primitives, despite the identified hierarchy in post-stroke performance.

The degradation hierarchy in performing discrete and rhythmic movements is not unique to stroke patients. For instance, cerebellar patients are impaired in producing discrete movements but not rhythmic movements (Spencer et al. 2003). This demonstrates the prominent role of the cerebellum in representing the temporal goal of discrete movements (Spencer et al. 2003, 2005). The temporal properties of rhythmic movements are, however, supposed to be emergent. Once the rhythmic movement is initiated, the performance is probably controlled by other parameters governing other movement constraints, such as minimizing the jerk or spatial noise.

Together, these results support the results showing that discrete and rhythmic movements recruit different cortical and cerebellar networks during their execution (Schaal et al. 2004). This reinforces the consensus claiming that rhythmic and discrete movements form two fundamental and distinct motor primitives.

On top of that, planning is an important step in goal-oriented movements, both discrete and rhythmic. Planning precedes execution, and requires the assessment of the movement (energetic) cost in order to select an appropriate control policy (Shadmehr and Krakauer 2008). This process likely takes place – at least partly – in the basal ganglia, an area being severely degraded in Parkinson’s disease (Mazzoni et al. 2007). Patients suffering from Parkinson’s disease display impairments in intensive and inter-segment coordinative aspects of both discrete and rhythmic movements, leading respectively to e.g. lower velocity peaks and decreased accuracy (Levy-Tzedek et al. 2011). This shows that, despite they form different motor primitives, discrete and rhythmic movements might also recruit similar mechanisms, for instance associated to movement planning.

Non-visually guided rhythmic movements are less affected than visually guided rhythmic movements

The non-visually guided rhythmic movements were less affected than the visually guided ones, so that the non-visually guided condition was the least affected among the three conditions tested. Although the number of velocity peaks was not significantly different between the paretic arms of the patients and the arms of control subjects in both rhythmic conditions, we observed a higher harmonicity of the paretic arm during the R-NT task than during the R-T task. Moreover, all patients but one (patient 7) who were affected in the R-T and/or D-T tasks performed the R-NT task like the healthy control group, at least regarding the PEAK metric during the central phase of the movement.

Executing a rhythmic movement under visual guidance recruits an extended visuomotor cortical network (Desmurget et al. 1999, 2001; Hanakawa et al. 2008; Andersen and Cui 2009; Glover et al. 2012), while this activation decreases when visual feedback is removed (Ronsse et al. 2011). Any potential damage in this pathway seems to preserve the capacity to execute non-visually guided rhythmic movement with limited kinematic impairments.

Impairment hierarchy shows a possible role for spinal oscillators in rhythmic upper limb movements

The observation that rhythmic arm movements recruit fewer cortical areas could be connected with the principle

of central pattern generators (CPGs). CPGs were identified as neural oscillators capable of producing a periodic output while receiving no periodic input (Brown 1914; Shik et al. 1966; Marder and Bucher 2001; Ijspeert 2008). Locomotor CPGs are located – at least partly – at the spinal level, as revealed by studies in nonprimates and humans (Cohen et al. 1988; Collins and Richmond 1994; Dimitrijevic et al. 1998; Duysens and Van de Crommert 1998; Swinnen 2002; Kawashima et al. 2005). More recently, the concept of CPGs has also been extended to rhythmic movements in the upper extremities (Dietz, 2002; Zehr and Duysens, 2004; Zehr et al., 2004; White et al., 2008; Ronsse et al., 2009), suggesting the presence of similar lower-level, i.e., spinal, circuitries for voluntary rhythmic arm movements.
Our data revealed that the smoothness of rhythmic movements is preserved to a larger extent than discrete movements after a stroke, possibly associated with the fact that rhythmic arm movements might be partly governed by low-level CPGs. As the spinal contribution to rhythmic arm movement would remain accessible after a stroke (Zehr et al. 2012), smooth rhythmic movements – once initiated – could be performed mainly by relying on those undamaged low-level circuitries. In contrast, discrete movements require the recruitment of a broad cortical and cerebellar network, spanning over areas silent during rhythmic movement production (Schaal et al. 2004).

This hierarchy of impairment could also account for the reported findings on asymmetric transfer between rhythmic and discrete movements (Ikegami et al. 2010). In a motor learning task, these authors reported that rhythmic movements training do not transfer to discrete movements, while in contrast discrete movements training does transfer, as least partially. Again, this suggests that the cortical substrate involved in discrete motor learning includes the one recruited during rhythmic movements, but not the other way around.

Limitations

In this paper, we compared two naturally-induced movement types (rhythmic vs. discrete movements) by asking subjects to perform the same task but with different IDs. In particular, the discrete movement was induced by making the task “more difficult,” i.e., forcing the subject to stop on the targets, although this was not explicitly requested.

The main limitation of this study is, consequently, that we did not add an additional discrete task with the same ID as during the rhythmic task, i.e. by explicitly asking the participants to stop on the targets. Our intention was rather to induce rhythmic and discrete movements in an "ecological" (or implicit) way, as happens in daily life contexts. Participants produced rhythmic and discrete movements, although they received the exact same instructions for both tasks. Forcing discrete movements in a task having an ID calling for rhythmic movements would have broken this implicit context and strongly impacted the instructions to be delivered. In particular, we did not have to ask the participants to spend a specific duration on the targets (the so-called dwell time): this was, again, naturally happening due to the movement strategy they selected.

Interestingly, we reported an impairment in the D-T task in both the central and reversal phases of the movement; this suggests that this type of movement requires a planning step that embraces the whole movement duration (Andersen and Cui 2009; Glover et al. 2012), and that this whole planning process is affected by a stroke insult. However, whether these results would be observed with discrete movements produced with the explicit instruction to stop on the targets (i.e., potentially with the same ID as our rhythmic movements) or without visual targets is still an open question.

Finally, our protocol was made so that there were two simultaneous changes in the design of sequences: half of the participants performed the sequence with the reversed order of conditions and arms with respect to the other half. It would have been preferable to fully randomize the sequence of conditions and arms for each participant. Indeed, with this sequencing, neither the arm sequence effect nor the condition order effect can be studied, as they may cancel each other out.

Potential therapeutic interest

Currently, classical upper-limb therapy focuses on intensive, task-specific, and context-specific movement training, which is composed of mainly discrete movements (Langhorne et al. 2011). Our data confirms that these movements are the most affected ones and confirms the importance of intensively training these movements after stroke.

However, if rhythmic movements are affected by a stroke – as we report in the present paper for a majority of our patients – they should also be included in the post-stroke therapy, in order to reach proper motor recovery of rhythmic movements themselves. Several complex daily life movements are based on the combination of rhythmic and discrete movements, like handwriting, scrabbling, hammering, knitting, sweeping a table, and playing the piano (Sternad and Dean 2003). Recovering such coordinated movements after a stroke would require the recovery of the combined execution of the independent motor primitives. Indeed, since rhythmic and discrete movements are – at least partially – controlled by independent neural circuitries and form two different primitives, both need to be trained to recover a complete motor repertoire (Sternad and Dean 2003; Schaal et al. 2004; Haiss and Schwarz 2005; Ikegami et al. 2010; Howard et al. 2011).

Moreover, assuming that rhythmic movements are less affected than discrete ones, a progression in the exercises could be proposed from rhythmic to discrete movements. It might be feasible to build on the fact that rhythmic movements are lower in hierarchy and hence are more frequently intact. If so, discrete elements could be combined with rhythmic movements, leveraging the execution of movements with a higher degree of impairment to those which are performed more stably.

Experimental paradigms including both movement types, like those performed by Sternad et al. (2000) for single-joint movements or Sternad and Dean (2003) for two-joint movements, are viable candidates.

Finally, several previous studies showed that rhythmic arm cycling reduces spasticity and improves the range of motion and strength (Barbeau and Visintin 2003; Diserens et al. 2007; Zondervan et al. 2013a, 2013b).

Moreover, bilateral arm training with rhythmic auditory cueing (Whitall et al. 2000; Luft et al. 2004) was shown to improve motor functions beyond those being trained, as captured by the improvement of several functional post-stroke assessment scales (FMA, Wolf Motor Function Test, daily live function, strength, and range of motion). This tends to suggest that performing unilateral rhythmic movements improves the general upper-limb performances after stroke.

In conclusion, the present paper studied rhythmic versus discrete movements in stroke patients to provide new insights on the neural organization of those two fundamental movements. These findings further suggest training rhythmic movements *in addition* to discrete movements during therapy to maximize post-stroke motor recovery.

Conflicts of interest

The authors declare no competing financial interests.

Acknowledgements

The authors would like to thank Catherine Rasse for her support with the statistics, the subjects for their availability to participate in the study, and the physiotherapists who helped in recruitment of the patients.

Funding

This work was supported by the FRIA (Fonds pour la Recherche dans l'Industrie et l'Agriculture) and by the "Fondation van Goethem Brichant."

References

Andersen RA, Cui H. Intention, Action Planning, and Decision Making in Parietal-Frontal Circuits. *Neuron* 63: 568–583, 2009.

Balasubramanian S, Melendez-Calderon A, Burdet E. A robust and sensitive metric for quantifying movement smoothness. *Biomed Eng IEEE Trans On* 59: 2126–2136, 2012.

Barbeau H, Visintin M. Optimal outcomes obtained with body-weight support combined with treadmill training in stroke subjects. *Arch Phys Med Rehabil* 84: 1458–1465, 2003.

Brown TG. On the nature of the fundamental activity of the nervous centres; together with an analysis of the conditioning of rhythmic activity in progression, and a theory of the evolution of function in the nervous system. *J Physiol* 48: 18-46, 1914.

Buchanan JJ, Park J-H, Shea CH. Target width scaling in a repetitive aiming task: switching between cyclical and discrete units of action. *Exp Brain Res* 175: 710–725, 2006.

Cirstea M, Levin MF. Compensatory strategies for reaching in stroke. *Brain* 123: 940–953, 2000.

Cohen AH, Rossignol S, Grillner S. Neural control of rhythmic movements in vertebrates. .

Collins JJ, Richmond S. Hard-wired central pattern generators for quadrupedal locomotion. *Biol Cybern* 71: 375–385, 1994.

Dagnelie P. *Statistique théorique et appliquée. 1, 1,*. Bruxelles: De Boeck, 2013.

Desmurget M, Epstein CM, Turner RS, Prablanc C, Alexander GE, Grafton ST. Role of the posterior parietal cortex in updating reaching movements to a visual target. *Nat Neurosci* 2: 563–567, 1999.

Desmurget M, Gréa H, Grethe JS, Prablanc C, Alexander GE, Grafton ST. Functional anatomy of nonvisual feedback loops during reaching: a positron emission tomography study. *J Neurosci* 21: 2919–2928, 2001.

Dietz V. Proprioception and locomotor disorders. *Nat Rev Neurosci* 3: 781–790, 2002.

Dimitrijevic MR, Gerasimenko Y, Pinter MM. Evidence for a spinal central pattern generator in humansa. *Ann N Y Acad Sci* 860: 360–376, 1998.

Dipietro L, Krebs HI, Fasoli SE, Volpe BT, Hogan N. Submovement changes characterize generalization of motor recovery after stroke. *Cortex* 45: 318 – 324, 2009.

Diserens K, Perret N, Chatelain S, Bashir S, Ruegg D, Vuadens P, Vingerhoets F. The effect of repetitive arm cycling on post stroke spasticity and motor control: repetitive arm cycling and spasticity. *J Neurol Sci* 253: 18–24, 2007.

Duysens J, Van de Crommert HW. Neural control of locomotion; Part 1: The central pattern generator from cats to humans. *Gait Posture* 7: 131–141, 1998.

Fitts PM. The information capacity of the human motor system in controlling the amplitude of movement. *J Exp Psychol 47*(6): 381,1954.

Fugl-Meyer A, Jääskö L, Leyman I, Olsson S, Steglind S. The post-stroke hemiplegic patient. 1. a method for evaluation of physical performance. *Scand J Rehabil Med* 7: 13–31, 1974.

Gilliaux M, Lejeune T, Detrembleur C, Sapin J, Dehez B, Stoquart G. A robotic device as a sensitive quantitative tool to assess upper limb impairments in stroke patients: a preliminary prospective cohort study. *J Rehabil Med* 44: 210–7, 2012.

Gilliaux M, Lejeune TM, Detrembleur C, Sapin J, Dehez B, Selves C, Stoquart G. Using the robotic device REAplan as a valid, reliable, and sensitive tool to quantify upper limb impairments in stroke patients. *J Rehabil Med* 46: 00–00, 2014a.

Gilliaux M, Renders A, Dispa D, Holvoet D, Sapin J, Dehez B, Detrembleur C, Lejeune TM, Stoquart G. Upper Limb Robot-Assisted Therapy in Cerebral Palsy: A Single-Blind Randomized Controlled Trial. *Neurorehabil. Neural Repair* (July 11, 2014b). doi: 10.1177/1545968314541172.

Giszter SF. Motor primitives-new data and future questions. *Curr Opin Neurobiol* 33: 156-165, 2015.

Glover S, Wall MB, Smith AT. Distinct cortical networks support the planning and online control of reaching-to-grasp in humans: Cortical planning and control. *Eur J Neurosci* 35: 909–915, 2012.

Goto Y, Jono Y, Hatanaka R, Nomura Y, Tani K, Chujo Y, Hiraoka K. Different corticospinal control between discrete and rhythmic movement of the ankle. *Front Hum Neurosci* 8, 2014.

Gowland C, Basmajian JV, Plews N, Burcea I, others. Agonist and antagonist activity during voluntary upper-limb movement in patients with stroke. *Phys Ther* 72: 624–633, 1992.

Guiard Y. On Fitts's and Hooke's laws: Simple harmonic movement in upper-limb cyclical aiming. *Acta Psychol (Amst)* 82: 139–159, 1993.

Haiss F, Schwarz C. Spatial segregation of different modes of movement control in the whisker representation of rat primary motor cortex. *J Neurosci* 25: 1579–1587, 2005.

Hanakawa T, Dimyan MA, Hallett M. Motor Planning, Imagery, and Execution in the Distributed Motor Network: A Time-Course Study with Functional MRI. *Cereb Cortex* 18: 2775–2788, 2008.

Hogan N, Sternad D. On rhythmic and discrete movements: reflections, definitions and implications for motor control. *Exp Brain Res* 181: 13–30, 2007.

Hogan N, Sternad D. Sensitivity of smoothness measures to movement duration, amplitude, and arrests. *J Mot Behav* 41: 529–534, 2009.

Hogan N, Sternad D. Dynamic primitives of motor behavior. *Biol Cybern* 106: 727-739, 2012.

Hogan N, Sternad D. Dynamic primitives in the control of locomotion. *Front Comput Neurosci* 7: 71, 2013.

Howard IS, Ingram JN, Wolpert DM. Separate representations of dynamics in rhythmic and discrete movements: evidence from motor learning. *J Neurophysiol* 105: 1722–1731, 2011.

Ijspeert AJ. Central pattern generators for locomotion control in animals and robots: a review. *Neural Netw* 21: 642–653, 2008.

Ikegami T, Hirashima M, Taga G, Nozaki D. Asymmetric transfer of visuomotor learning between discrete and rhythmic movements. *J Neurosci* 30: 4515–4521, 2010.

Kamper DG, McKenna-Cole AN, Kahn LE, Reinkensmeyer DJ. Alterations in reaching after stroke and their relation to movement direction and impairment severity. *Arch Phys Med Rehabil* 83: 702–707, 2002.

Kawashima N, Nozaki D, Abe MO, Akai M, Nakazawa K. Alternate leg movement amplifies locomotor-like muscle activity in spinal cord injured persons. *J Neurophysiol* 93: 777–785, 2005.

Krebs HI, Hogan N, Volpe BT, Aisen ML, Diels C. Overview of clinical trials with MIT-MANUS: a robot-aided neuro-rehabilitation facility. *Technol Health Care* 7: 419–423, 1999.

Langhorne P, Bernhardt J, Kwakkel G. Stroke rehabilitation. *The Lancet* 377: 1693–1702, 2011.

Levy-Tzedek S, Krebs HI, Arle JE, Shils JL, Poizner H. Rhythmic movement in Parkinson's disease: effects of visual feedback and medication state. *Exp Brain Res* 211: 277–286, 2011.

Levy-Tzedek S, Krebs HI, Song D, Hogan N, Poizner H. Non-monotonicity on a spatio-temporally defined cyclic task: evidence of two movement types? *Exp Brain Res* 202: 733–746, 2010.

Luft AR, McCombe-Waller S, Whitall J, Forrester LW, Macko R, Sorkin JD, Schulz JB, Goldberg AP, Hanley DF. Repetitive bilateral arm training and motor cortex activation in chronic stroke: a randomized controlled trial. *Jama* 292: 1853–1861, 2004.

Marder E, Bucher D. Central pattern generators and the control of rhythmic movements. *Curr Biol* 11: R986–R996, 2001.

Mazzoni P, Hristova A, Krakauer JW. Why don't we move faster? Parkinson's disease, movement vigor, and implicit motivation. *J Neurosci* 27: 7105-7116, 2007.

Van Mourik AM, Beek PJ. Discrete and cyclical movements: unified dynamics or separate control? *Acta Psychol (Amst)* 117: 121–138, 2004.

Nozaki D, Kurtzer I, Scott SH. Limited transfer of learning between unimanual and bimanual skills within the same limb. *Nat Neurosci* 9: 1364–1366, 2006.

Rohrer B, Fasoli S, Krebs HI, Hughes R, Volpe B, Frontera WR, Stein J, Hogan N. Movement smoothness changes during stroke recovery. *J Neurosci* 22: 8297–8304, 2002.

Ronsse R, Puttemans V, Coxon JP, Goble DJ, Wagemans J, Wenderoth N, Swinnen SP. Motor learning with augmented feedback: modality-dependent behavioral and neural consequences. *Cereb Cortex* 21: 1283–1294, 2011.

Ronsse R, Sternad D, Lefevre P. A computational model for rhythmic and discrete movements in uni- and bimanual coordination. *Neural Comput* 21: 1335–1370, 2009.

De Rugy A, Sternad D. Interaction between discrete and rhythmic movements: reaction time and phase of discrete movement initiation during oscillatory movements. *Brain Res* 994: 160–174, 2003.

Schaal S, Kotosaka S, Sternad D. Nonlinear dynamical systems as movement primitives [Online]. In: *IEEE International Conference on Humanoid Robotics*, p. 1–11. http://wwwiaim.ira.uka.de/users/rogalla/WebOrdnerMaterial/schaal-ICHR2000.pdf [17 Feb. 2015].

Schaal S, Sternad D, Osu R, Kawato M. Rhythmic arm movement is not discrete. *Nat Neurosci* 7: 1136–1143, 2004.

Shadmehr R, Krakauer JW. A computational neuroanatomy for motor control. *Exp Brain Res* 185: 359–381, 2008.

Shik ML, Severin FV, Orlovsky GN. Control of walking and running by means of electric stimulation of the midbrain. *Biofizika* 11: 659-666, 1966.

Simkins M, Jacobs AB, Rosen J. Rhythmic affects on stroke-induced joint synergies across a range of speeds. *Exp Brain Res* 229: 517–524, 2013.

Smits-Engelsman B, Swinnen S, Duysens J. The advantage of cyclic over discrete movements remains evident following changes in load and amplitude. *Neurosci Lett* 396: 28–32, 2006.

Spencer RMC, Ivry RB, Zelaznik HN. Role of the cerebellum in movements: control of timing or movement transitions? *Exp Brain Res* 161: 383–396, 2005.

Spencer RM, Zelaznik HN, Diedrichsen J, Ivry RB. Disrupted timing of discontinuous but not continuous movements by cerebellar lesions. *Science* 300: 1437–1439, 2003.

Sternad D, Dean WJ. Rhythmic and discrete elements in multi-joint coordination. *Brain Res* 989: 152–171, 2003.

Sternad D, Dean WJ, Schaal S. Interaction of rhythmic and discrete pattern generators in single-joint movements. *Hum Mov Sci* 19: 627–664, 2000.

Sternad D, Marino H, Charles SK, Duarte M, Dipietro L, Hogan N. Transitions between discrete and rhythmic primitives in a unimanual task. *Front Comput Neurosci* 7, 2013.

Swinnen SP. Intermanual coordination: from behavioural principles to neural-network interactions. *Nat Rev Neurosci* 3: 348–359, 2002.

Whitall J, Waller SM, Silver KH, Macko RF. Repetitive bilateral arm training with rhythmic auditory cueing improves motor function in chronic hemiparetic stroke. *Stroke* 31: 2390–2395, 2000.

White O, Bleyenheuft Y, Ronsse R, Smith AM, Thonnard J-L, Lefevre P. Altered gravity highlights central pattern generator mechanisms. *J Neurophysiol* 100: 2819–2824, 2008.

Zehr EP, Carroll TJ, Chua R, Collins DF, Frigon A, Haridas C, Hundza SR, Thompson AK. Possible contributions of CPG activity to the control of rhythmic human arm movement. *Can J Physiol Pharmacol* 82: 556–568, 2004.

Zehr EP, Duysens J. Regulation of arm and leg movement during human locomotion. *The Neuroscientist* 10: 347–361, 2004.

Zehr EP, Loadman PM, Hundza SR. Neural control of rhythmic arm cycling after stroke. *J Neurophysiol* 108: 891–905, 2012.

Zondervan DK, Palafox L, Hernandez J, Reinkensmeyer DJ. The resonating arm exerciser: design and pilot testing of a mechanically passive rehabilitation device that mimics robotic active assistance. *J Neuroeng Rehabil* 10: 39, 2013a.

Zondervan DK, Smith B, Reinkensmeyer DJ. Lever-actuated resonance assistance (LARA): A wheelchair-based method for upper extremity therapy and overground ambulation for people with severe arm impairment [Online]. In: *Rehabilitation Robotics (ICORR), 2013 IEEE International Conference on*. IEEE, p. 1–6. http://ieeexplore.ieee.org/xpls/abs_all.jsp?arnumber=6650400 [7 Oct. 2014b].

Figure legends

Fig. 1: Top: the REAplan robot, which was used as a measurement device. The white arrow denotes the movement direction that was studied in this experiment, i.e. forward-backward in the sagittal plane. Bottom: graphical interface (iv) shown to the patients when performing, with the right arm, (a) the discrete task with small targets (D-T), (b) the rhythmic task with large targets (R-T), and (c) the rhythmic task without targets (R-NT).

Fig. 2: Illustration of the reported metrics during the production of discrete (left) and rhythmic (right) movements. One period or two submovements are displayed. Top: the position profile is displayed with the amplitude (A) and duration (D) of the first movement. Bottom: the velocity profile is displayed with the mean velocity, the number of peaks in the velocity profile, and the dwell time. Below, the acceleration profile is displayed with the landmarks used to compute the harmonicity index (i.e., $\boldsymbol{a_{min}}$ and $\boldsymbol{a_{max}}$). The lowest panel displays the squared jerk, which was used to compute the LDJ by normalizing the surface under the squared jerk profile by $\boldsymbol{D^3/v_{mean}^2}$.

Fig. 3 : Typical traces of subject 1 (left) and patient 7's paretic side (right) during the rhythmic with target (R-T, top) and the discrete with target (D-T, bottom) tasks. The gray areas represent the phases of movement reversal.

Fig. 4 : Top: general performance metrics, i.e. dwell time, precision, mean velocity and movement amplitude. Bottom: smoothness metrics, i.e. number of peaks, LDJ during the complete movement and number of peaks during the movement reversal and during the central phase of the movement only. These results are reported at the population level for the paretic arms (black), the non-paretic arms (dark gray) and the control arms (light gray) during the three tasks (except for the precision which cannot be computed during the R-NT task since no target was displayed). The error-bars represent 1 standard error of the mean. The task-specific horizontal lines with a '*' symbol show the cases for which the paretic arm is significantly different from the control and the non-paretic arms. The upper horizontal lines with a '*' highlight when the smoothness of the tasks are significantly different from each other.

Fig. 5 : Harmonicity index *H* of the paretic arms (black), the non-paretic arms (dark gray) and the control arms (light gray) during the three tasks. The error-bars represent 1 standard error of the mean. The task-specific horizontal lines with a '*' symbol show the cases for which the paretic arm is significantly different from the control and the non-paretic arms. The upper horizontal lines with a '*' highlight when the tasks are significantly different from each other.

Fig. 6 : Classification of the patients according to their impairments in the R-NT, R-T and D-T task computed from the LDJ and peak metric during the complete movement (a, b, c and d) and during the central phase of the movement only (e and f). Panels 'a', 'c' and 'e' show a Venn diagram of the classification with a threshold set to 1 standard deviation of the control group. Panels 'b','d' and 'f' show the same patient distribution by varying the classification threshold from 0.5 to 2 standard deviations.

Table 1: Main characteristics of the patients and control subjects (FMA : Fugl-Meyer Assessment, SD: standard deviation, N/A: information not available)

Patient	Gender	age	Months post-stroke	Dominant hand	Paretic side	FMA	Type, location of lesion
1	F	41	60	R	R	41	N/A
2	M	50	4	R	L	12	Hemorrhagic, Sub-cortical
3	M	54	12	R	L	61	N/A
4	F	57	22	R	L	41	Ischaemic, cortical
5	F	58	11	R	L	22	Hemorrhagic, sub-cortical
6	M	39	36	R	R	66	N/A
7	M	63	3	R	L	47	Ischaemic, cortical and sub-cortical
8	F	57	8	R	R	57	Ischaemic, cortical
9	M	53	3	L	L	21	Ischaemic, cortical and sub-cortical
10	M	56	3	L	L	6	Ischaemic, Cortical and sub-cortical
11	M	58	10	R	R	52	Ischaemic, cortical

	Stroke	Control
Amount of subjects	11	11
Gender (Male/Female)	7/4	3/8

Age (SD)	53.3 (7.4) years	55 (13.2) years
Dominant hand (Left/Right)	2/9	2/9

Table 2: Group - arm interaction and Tukey HSD of the paretic vs. control arms and of the paretic vs. non-paretic arms in the PEAK and LDJ metric over the total movement, and in both phases of the movement (central and reversal phase).

	Paretic vs. Control		**Paretic vs. non-paretic**	
	Interaction group – task	**Tukey**	**Interaction group – task**	**Tukey**
PEAK total	$F_{(2,40)} = 17.5$, $p < 0.0001$	DT: **p < 0.0001**	$F_{(2,50)} = 14.3$, $p <0.0001$	DT: **p < 0.0001**
		RT: p = 0.68		RT: p = 0.63
		RNT: p = 1		RNT: p = 0.998
LDJ total	$F_{(2,40)} = 13.0$, $p < 0.0001$	DT: **p =0.0008**	$F_{(2,50)} = 0.69$, $p = 0.006$	DT: **p < 0.0001**
		RT: p = 0.11		RT: **p = 0.01**
		RNT: p = 0.93		RNT: p = 0.45
PEAK central	$F_{(2,40)} = 9.6$, $p = 0.0004$	DT: **p < 0.0001** RT: p = 0.99 RNT: p = 1	$F_{(2,50)} = 7.13$, $p = 0.0019$	**DT: p = 0.0002** RT: p = 0.99 RNT: p = 1
PEAK reversal	$F_{(2,40)} = 18.3$, $p < 0.0001$	DT: **p<0.0001** RT: p = 0.6 RNT: p = 1	$F_{(2,50)} = 15.1$, $p < 0.0001$	DT: **p<0.0001** RT: p = 0.32 RNT: p = 1

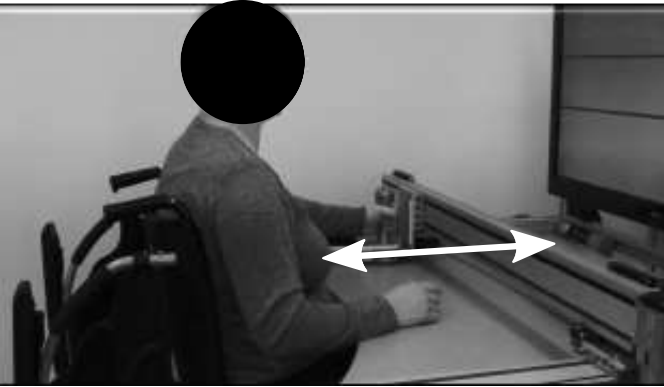

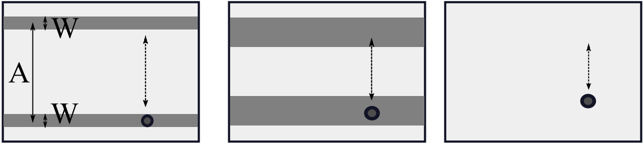

a) D-T b) R-T c) R-NT

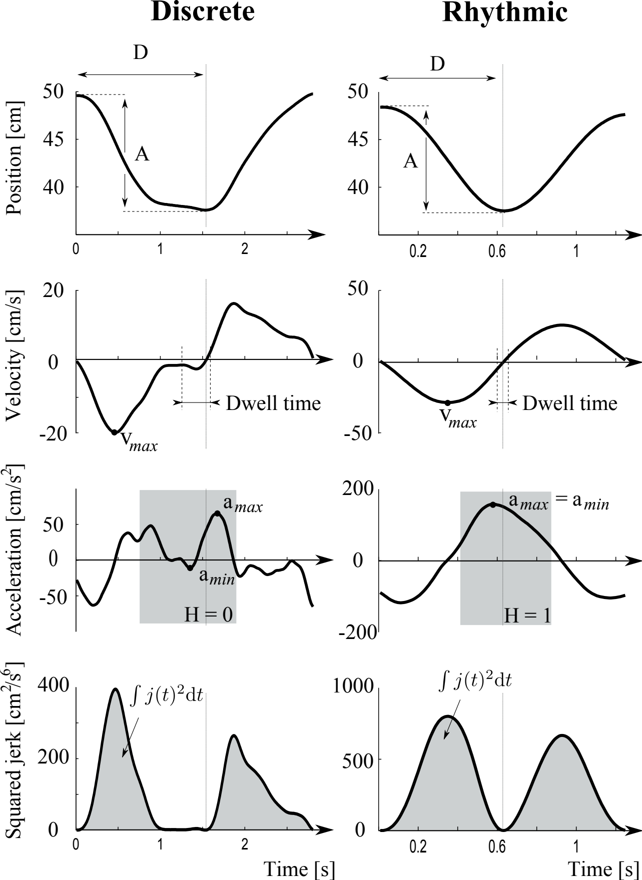

Discrete
Rhythmic
D
A
Position [cm]
50
45
40
0
1
2
0.2
0.6
1
Velocity [cm/s]
20
0
-20
50
-50
Dwell time
v_max
Acceleration [cm/s^2]
-50
200
-200
a_max
a_min
a_max = a_min
H = 0
H = 1
Squared jerk [cm^2/s^6]
400
200
1000
500
∫ j(t)^2 dt
Time [s]

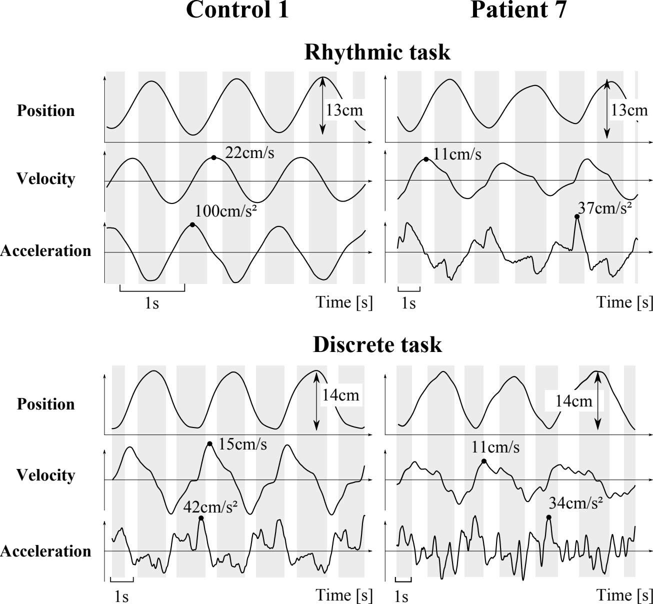

Control 1
Patient 7
Rhythmic task
Position
Velocity
Acceleration
13cm
22cm/s
100cm/s²
1s
Time [s]
13cm
11cm/s
37cm/s²
1s
Time [s]
Discrete task
Position
Velocity
Acceleration
14cm
15cm/s
42cm/s²
1s
Time [s]
14cm
11cm/s
34cm/s²
1s
Time [s]

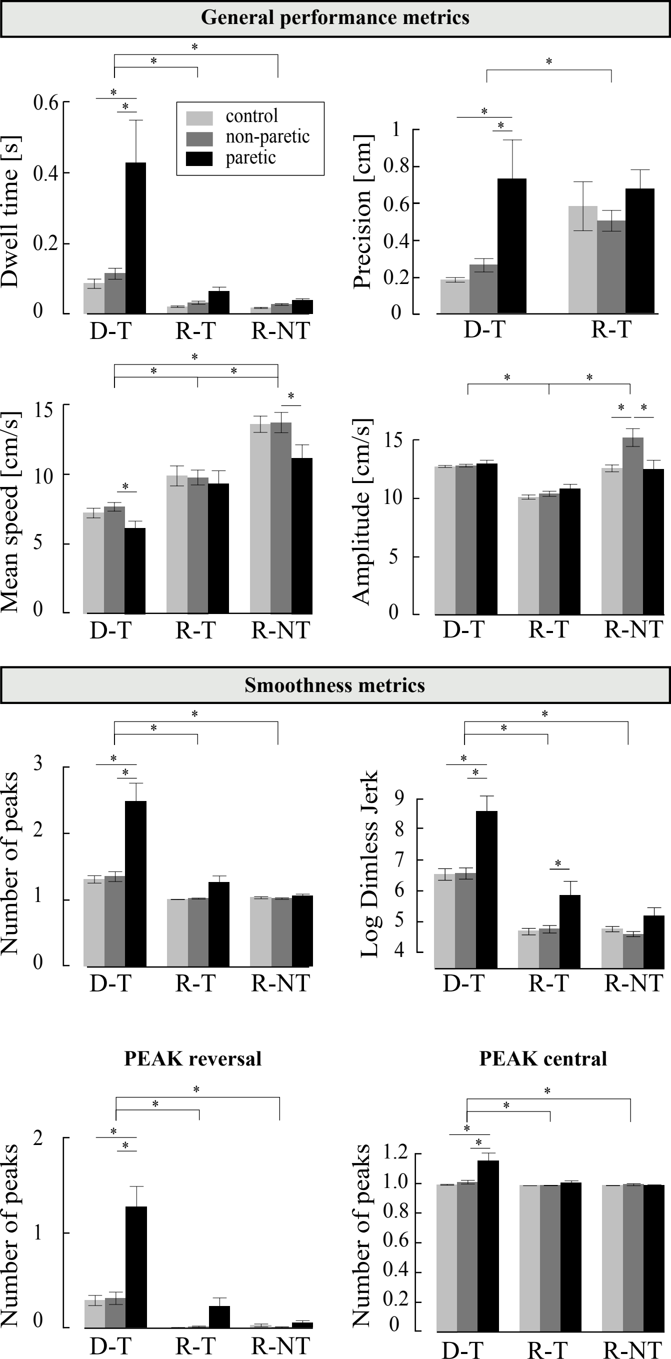
General performance metrics
control
non-paretic
paretic
Dwell time [s]
0.6
0.4
0.2
0
D-T
R-T
R-NT
Precision [cm]
1
0.8
0.6
0.4
0.2
0
Mean speed [cm/s]
15
10
5
Amplitude [cm/s]
Smoothness metrics
Number of peaks
3
2
1
Log Dimless Jerk
9
8
7
6
5
4
PEAK reversal
PEAK central
1.2
1.0
*

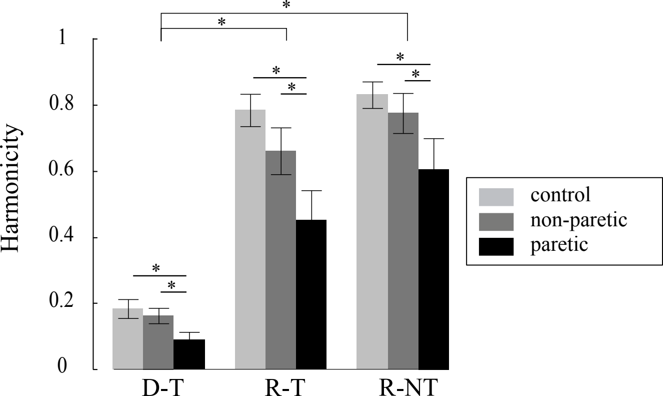

Harmonicity
1
0.8
0.6
0.4
0.2
0
D-T
R-T
R-NT
control
non-paretic
paretic
*

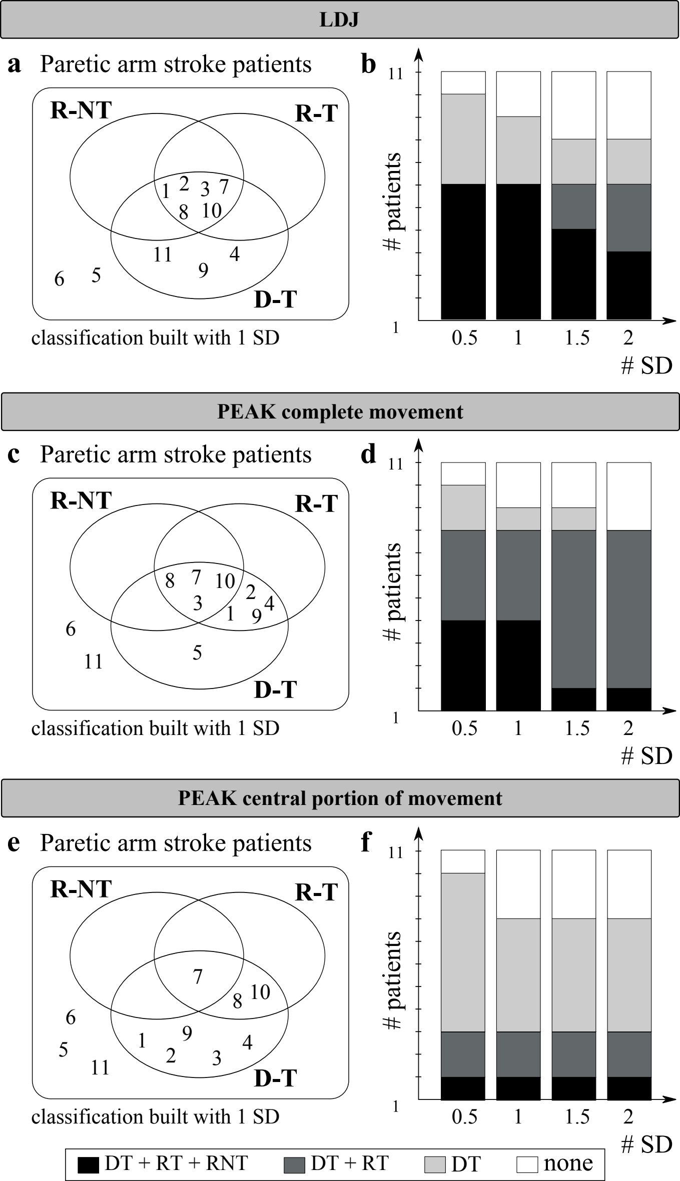

LDJ
a
Paretic arm stroke patients
R-NT
R-T
D-T
1 2 3 7 8 10
11 9 4
6 5
classification built with 1 SD
b
patients
11
1
0.5
1
1.5
2
SD
PEAK complete movement
c
Paretic arm stroke patients
R-NT
R-T
D-T
8 7 10 3
2 4 1 9
6 11
5
classification built with 1 SD
d
patients
11
1
0.5
1
1.5
2
SD
PEAK central portion of movement
e
Paretic arm stroke patients
R-NT
R-T
D-T
7
8 10
6 5 11
1 9 2 3 4
classification built with 1 SD
f
patients
11
1
0.5
1
1.5
2
SD
DT + RT + RNT
DT + RT
DT
none

Rhythmic arm movements are less affected than discrete ones after a stroke

P. Leconte, J.J. Orban de Xivry, G. Stoquart, T. Lejeune, and R. Ronsse
Université catholique de Louvain, 2015

Supplementary material: details of the mixed model equation

The mixed model equation that was used in our analyzes is the following:

$$\boldsymbol{Y} = \boldsymbol{X\beta} + \boldsymbol{Z\gamma} + \boldsymbol{\varepsilon}$$

where $\boldsymbol{Y}$ is the $n \times 1$ vector of responses (n being the number of observations), $\boldsymbol{X}$ is the $n \times p$ design matrix for the fixed effects (p being the number of variables, i.e. the factors and their interactions); $\boldsymbol{\beta}$ is a $p \times 1$ vector of unknown fixed effects with the design matrix $\boldsymbol{X}$**;** $\boldsymbol{Z}$ is the $n \times s$ design matrix for the random effects (with s being the number of subjects); $\boldsymbol{\gamma}$ is a $s \times 1$ vector of unknown random effects with the design matrix $\boldsymbol{Z}$**;** $\boldsymbol{\varepsilon}$ is a $n \times 1$ vector of unknown random errors. Note that both $\boldsymbol{\gamma}$ and $\boldsymbol{\varepsilon}$ follow a Gaussian distribution, i.e. $\boldsymbol{\gamma} \sim \boldsymbol{N}(\boldsymbol{0}, \boldsymbol{G})$ with $\boldsymbol{G}$ being a $s \times s$ diagonal matrix with identical entries for each effect, and $\boldsymbol{\varepsilon} \sim \boldsymbol{N}(\boldsymbol{0}, \sigma^2 \boldsymbol{I_n})$ with $\boldsymbol{I_n}$ being the $n \times n$ identity matrix.

The covariance structure for this model is also called a "variance component structure". A distinct variance component is assigned for each of the random effects (here, one single random effect, i.e. the subject effect), and the covariances are null.

Reference: SAS/STAT 9.2 User's Guide, 2008, p.3955